Using Lysine-Reactive Fluorescent Dye for Surface Characterization of a
Monoclonal Antibody

BY

Ming Lei

Submitted to the graduate degree program in Pharmaceutical Chemistry and the
Graduate Faculty of the University of Kansas in partial fulfillment of the
requirements for the degree of Master of Arts.

_____

Chairperson: Christian Schöneich

_____

John Stobaugh

_____

Yung-Hsiang Kao

Date Defended: December, 8th ,2014

The Thesis Committee for Ming Lei certifies that this is the approved version of the following thesis:

Using Lysine-Reactive Fluorescent Dye for Surface Characterization of a Monoclonal Antibody

_____

Chairperson: Christian Schöneich

Date approved:

ABSTRACT

The last decade has witnessed a rapid growth in the development of protein pharmaceuticals for diagnostic and therapeutic purposes. The biopharmaceutical industry increasingly demands thorough characterization of protein conformation and conformational dynamics to ensure product quality and consistency. Here we present a chromatography-based method that is able to characterize protein conformation and conformational dynamics at peptide level resolution in a high-throughput manner. The surface lysine residues of the protein were labeled with a fluorescent dye prior to trypsin and Glu-C digestion. The resulting peptide maps were monitored by fluorescence detection and the peak areas of the respective peptides were normalized to protein concentration. The normalized fluorescence peak area for a specific peptide represents the individual lysine solvent accessibility. A higher normalized fluorescence peak area indicates higher solvent accessibility at a specific site. The identity of the peak of interested was determined by LC-MS/MS analysis. We first demonstrated this method is suitable for probing protein surface/conformation by studying the effect of deglycosylation on a recombinant monoclonal antibody (mAb), IgG 1. The results from this method were consistent with previous results obtained by H/D-exchange. We then applied our method to study the interaction of the mAb with a common excipient, polysorbate-20 (PS-20). The interaction between PS-20 and the mAb was generally weak. The presence of PS-20 increased the fluorescent labeling of several lysine residues on the mAb. These lysine residues localized near the protein domains of relatively high hydrophobicity. This result provides a first insight into PS-20-mAb interaction at peptide level resolution.

ACKOWLEDGEMENT

TABLE OF CONTENTS

INTRODUCTION

Proteins provide a wide array of functions in living organisms and are involved, e.g., in active transport processes, metabolism and immunity. Protein function is determined by protein structure and conformational dynamics where protein structure is defined as primary, secondary, tertiary and quaternary structure. The primary structure involves the amino acid sequence and its post-translational modifications such as, e.g., oxidation, deamidation and phosphorylation[1]. Higher-order structures of proteins depend on the conformation of local substructures, the global structures of protein molecules and the assembly of multi-subunit proteins[2]. Importantly, proteins are dynamic because either the entire molecule and/or its local substructures may open, close and tumble on various time scales[3]. In the biopharmaceutical industry, the conformation and conformational dynamics of proteins are important for product quality and comparability[3-6]. Therapeutic protein can be produced through multiple means, such as recombinant, purified or the combination of the two. As a pharmaceutical product, the quality of therapeutic proteins is strictly controlled and monitored. The control system of each therapeutic protein is comprised of many assays that ensure the whole production, purification, formulation and filling processes are performing as expected. The quality of therapeutic protein is defined in many facets. The quality attributes that affect the activity and/or safety of the therapeutic protein are called critical quality attributes (CQAs)[7,8]. Protein higher-order structure can be one of or closely linked to the CQAs. For example, scrambled disulfide bonds can lead to altered higher-order structure that may affect protein's safety and efficacy profile, thus is usually a CQA[9,10]. Scrambled disulfide bond can usually be detected by LC-MS/MS that requires method development for each specific molecule. However, a method that directly detects higher-order structure change regardless of the source is

more universal that eliminates the need of method development for each modification and molecule.

Studying the dynamics and higher order structure of proteins also offers insight into product quality consistency, such as batch-to-batch consistency and stability[3,11]. The information about the conformation and conformational dynamics of proteins will also assist in determining whether a variant would have safety or efficacy issues.

The characterization of conformation and conformational dynamics of proteins usually requires sophisticated methodologies such as nuclear magnetic resonance spectroscopy (NMR) [12,13], X-ray crystallography[14,15], Fourier transform infrared spectroscopy (FT-IR)[16-18] and circular dichroism (CD)spectroscopy[19,20]. Among these, NMR and X-ray crystallography offer structural determination and excellent resolution but involve intensive sample preparation, analysis and data interpretation[21]. NMR usually requires isotopically labeled proteins in relatively large quantity while X-ray crystallography requires crystallized protein that is not always available. The other two techniques (FT-IR and CD) do not have such a high requirement on sample but lack residue-level structural information[21].

In most of the situations encountered in the biopharmaceutical industry, only structural comparison rather than structural determination is needed[22,23]. Several analytical methodologies have been developed to serve that increasing demand, including hydrogen/deuterium exchange mass spectrometry (H/DX-MS)[22,24-27] and chemical footprinting methods[25,28-32]. Both of these methodologies can offer peptide or residue level resolution for evaluating structural and dynamic differences between two samples. However, these methods require specialized equipment and

high-resolution MS. Additionally, the data analysis is often time-consuming (1-2 days per sample[22]) and requires specialized software.

Here we describe an HPLC-based technology to characterize the conformation and conformational dynamics of a protein. The method can be used in a high throughput manner and does not require specialized software. This technology involves labeling the solvent-accessible lysines with a fluorescent dye in buffer and then enzymatically digesting the sample. The peptide maps are monitored both by UV- and fluorescence detection, and the fluorescence peak area normalized to protein concentration. The normalized fluorescence peak area corresponds to the local solvent accessibility of a specific lysine residue, and can thus, be used to compare the conformation and dynamics of two protein. We demonstrated the utility of this method by assessing the effect of deglycosylation on a recombinant mAb (IgG1). Our results are largely consistent with previous conformational studies based on H/DX-MS. We then applied this method to study the interaction between mAb and polysorbate 20 sorbitan monolaureate (PS-20). PS-20 is a widely used excipient in therapeutic protein formulations to reduce protein aggregation during production and shipping [33] [34] [35] [36] and to reduce protein adsorption on glass surfaces [37]. Its interaction with protein had been studied by means of CD spectroscopy, isothermal titration calorimetry (ITC) and tryptophan fluorescence [42,43]. The methodology described here offers an opportunity to gain insight into the interactions between a mAb and PS-20 on a peptide level for the first time.

Overall, the results from this study suggest that this protein surface lysine fluorescent labeling method is capable of detecting protein conformation and dynamics differences at the peptide level without the requirement of sophisticated instrumentation or specialized software. This methodology is, therefore, amenable for high throughput analysis.

EXPERIMENTAL SECTION

Materials

Alexa Fluor® 350 SE was purchased from Life Technologies® (Carlsbad, CA). Dithiothreitol (DTT), Tris (2-carboxyethyl)phosphine hydrochloride (TCEP-HCl), iodoacetic acid sodium salt (IAA), guanidine hydrochloride, acetonitrile (ACN), methanol, polysorbate-20 (PS-20) and trifluoroacetic acid (TFA) were obtained from Sigma-Aldrich® (St. Louis, MO). PNGase F was purchased from Prozyme® (San Diego, CA). Trypsin, sequencing grade was acquired from Promega® (Madison, WI) while Glu-C was obtained from Roche® Diagnostics (Indianapolis, IN). The monoclonal antibody 1 (mAb 1) used in the experiments was generated at Genentech, Inc..

Protein denaturation, reduction and digestion

Labeled protein samples were diluted 6-fold using 8 M guanidine-HCl. The pH of the solution was adjusted to 7.5 with 1M Tris prior to the addition of 12 µl of 1 M DTT to each sample to reduce the disulfide bonds; the samples were incubated at 37°C for 1 hr. After reduction by DTT, 15 µl of 2.9 M IAA were added to each sample to alkylate free cysteine residues. The remaining IAA was quenched by addition of 30 µl of 1 M DTT to each sample after an incubation period of 15 min at 37°C. The samples were then buffer exchanged into 10 mM phosphate buffer, pH 7.5, employing NAP-5 columns (GE healthcare lifesciences, Piscataway, NJ). Subsequently, a stock solution of 1 mg/ml Glu-C was added to each sample to acquire a final mAb1:Glu-C ratio of 40 : 1. The samples were incubated at room temperature for 18 hr. After completion of the Glu-C digestion, a stock solution of 1 mg/ml trypsin was added to samples to attain an mAb1:trypsin ratio of 40: 1. The samples were then incubated at 37°C for 2 hr. The digestion was quenched by addition of 20 µl of 10% TFA.

Deglycosylation

The mAb1 was buffer exchanged and diluted to 5 mg/mL with 10 mM phosphate buffer, pH 7.5. Approximately 20 mU PNGase F were added to the mAb1 solution and the samples incubated at 37^0C overnight. A control sample was prepared by incubation of mAb-1 at $37^°$C overnight in the absence of PNGase F.

Preparation of samples containing polysorbate-20

A stock solution of PS-20 was prepared at 10% (w/w) in 10 mM phosphate buffer, pH 7.5. Different volumes of the PS-20 stock solution were added to solutions of 5 mg/mL mAb1 in 10 mM phosphate buffer, pH 7.5, so that the final PS-20 levels were 0.01%, 0.05%, 0.1% and 0.5% (w/v). The PS-20 containing samples were incubated at room temperature for 1 hr before they were subjected to surface lysine fluorescent labeling followed by denaturation, reduction and digestion as described above.

Reverse-phase HPLC analysis of dye hydrolysis

An Agilent® 1290 HPLC system equipped with a fluorescence detector was connected to an Agilent® Poroshell 120 SB-C18 column (4.6 x 75 mm, 2.7 μm, pore size 120 Å). The mobile phases were methanol (A) and water (B). A linear gradient changed the content of mobile phase B from 20-100% within 5 min. The flow rate was 1 ml/min and the injection volume was 1 μL, with the column temperature set to 45 $^°$C. The excitation and emission wavelengths were 350 nm and 490 nm.

Size-exclusion HPLC analysis

A Waters® 2796 HPLC system equipped with a UV detector was connected to a TSK G3000SWXL column (7.8 x 300 mm; TOSOHAAS®). The mobile phase was 0.2 M potassium phosphate buffer, pH 6.2. The sample was analyzed under isocratic conditions at a flow rate of

0.5 mL/min for 30 min. The injection volume was 10 µL and the column temperature was at ambient.

Reverse-phase HPLC conditions for peptide mapping

A Waters[®] 2796 HPLC system or equivalent HPLC systems equipped with UV and fluorescent detectors was connected to a Phenomenex Luna[®] C18 column (2.1 x 250 mm, 3.5 µm, 300 Å). The mobile phases were 0.1 % TFA in water (A) and 0.08 % TFA in acetonitrile (B). The column was conditioned with 1% B for 3 min. A linear gradient program consisted of the following steps: 3 min, 1% B; 13 min, 10% B; 90 min, 30% B; 153 min 45% B; 160 min, 95% B; 165 min, 45% B; 168 min, 1% B; 180 min, 1% B. The flow rate was 0.25 ml/min and the injection volume was 50 µL. The oven temperature was kept at 60 $^{\circ}$C. The excitation and emission wavelengths used were 350 nm and 490 nm for Alexa Fluor® 350.

HPLC-MS/MS analysis

HPLC-MS/MS data were acquired on an Orbitrap® XL instrument (Thermo Scientific, Waltham, MA) interfaced with an Agilent® 1200 HPLC system. The chromatography conditions applied were the same as described above for peptide mapping. The MS data were acquired over the range between 500 and 2000 m/z. The ions with top 5 abundances were selected for MS/MS fragmentation analysis.

MS analysis of non-digested (intact) protein

The molecular weights of protein samples were measured by an Agilent® 6210 Series HPLC-Chip/TOF MS system. For intact mass measurement, the sample was diluted to 1 mg/mL by mobile phase A (see below). For mass measurement after disulfide reduction, the samples were incubated with 1 M TCEP-HCl for 10 min at room temperature before dilution to 1 mg/mL with

mobile phase A. The HPLC-chip consisted of a desalting column and a C18 analytical column. A gradient was delivered at 0.4 µL /min flow rate using 0.1% formic acid in water (mobile phase A) and 0.1% formic acid in acetonitrile (mobile phase B). A linear gradient was run from 10% B to 70% B within 8 min. A total of 5 ng protein was loaded onto the column and analyzed in the range of 500-3000 m/z.

MS data analysis

MS data for intact and reduced mAb1 were processed and deconvoluted using the MassHunter[®] Workstation B.06.00 (Agilent[®]). The deconvolution mass range was 130k-160k Da for intact protein samples and 40k-70k Da for reduced protein samples. The HPLC-MS/MS data were analyzed by ProteomeDiscoverer 3.1 [®] (Thermo[®]). A fixed modification of carboxymethylation and customized optional modification of Alexa Fluore® 350 were included. Glu-C and trypsin combination enzymes were selected with up to two missed cleavages.

Surface Lysine Fluorescent Labeling

Monoclonal antibody-1 was buffer exchanged into 10 mM phosphate buffer, pH 7.5, to a final concentration of 5 mg/mL. A stock solution of 70 mM Alexa Fluor 350 SE in water was prepared, and added to the mAB1 samples such that the final ratio of dye:protein was 100:1. The samples were incubated at 37 °C for 1-5 min. At each time point, 100 µL of sample were withdrawn from the reaction tube and the derivatization reaction quenched with 20 µL 10% TFA. Labeled samples were then denatured and digested according to the protein digestion protocol described below.

RESULTS AND DISCUSSION

Method Development and Optimization for Protein Surface Lysine Fluorescent Labeling

Labeling efficiency

A commercially available fluorescent dye, Alexa Fluor® 350 SE (succinimidyl ester) was selected as the lysine labeling reagent. It offers a high fluorescence quantum yield and good water solubility, and presents a succinimidyl ester function that selectively reacts with primary amines. In order to optimize the conditions for protein surface lysine fluorescent labeling, we studied the effect of dye-to-protein ratio and reaction time on the labeling of mAb1. The goal was to minimize the reaction time to reduce potential structural changes induced by the labeling reaction, while achieving high labeling coverage at the same time.

It is known that dye hydrolysis may compete with lysine labeling[38]. Therefore, we first measured the rate of hydrolysis using a chromatography-based method. The dye was subjected to the same reaction conditions as encountered during the labeling reaction but without the presence of mAb1. The reaction mixture was sampled every 10 min by a HPLC auto-sampler for the duration of 120 min. The results (data not shown) showed that the hydrolysis reaction followed pseudo-first order kinetics, where <5% dye in the ester form remained after 120 min.

We then subjected mAb1 to reaction with Alexa Fluor 350 SE at dye-to-protein ratios of 40:1 and 100:1 and 37°C for 1-60 minutes. Aliquots of 100 µL were withdrawn from the reaction mixtures at 1, 2, 3, 5, 10, 20, 30 and 60 min and quenched with 10 µL of 10% TFA. The progress of lysine labeling was monitored at both dye-to-protein ratios by ESI-MS analysis. The labeling of one lysine residue gives rise to a mass shift of +295.01 Da. The relative abundance of protein species containing different numbers of labeled lysine residues was quantified through the peak heights of the respective MS signals. Interestingly, no apparent differences in average labeling

efficiencies were observed for the heavy chains (HC) of both the glycosylated (native) and decglycoslyated mAb1. The average number of labels per chain was calculated by multiplying the number of labels of a given peak by its % abundance in all detected peaks. The average number of labels on each chain at 1-60 min reaction time with 40:1 and 100:1 dye-to-protein ratios is shown in **Figure 1**. **Figures 1a and 1b** show that the average number of labels on the light chain (LC) and HC increases with reaction time for both dye-to-protein ratios. Higher labeling yields were detected for a dye-to-protein ratio of 100:1 compared to that of 40:1. The average number of labels incorporated into mAb1 increased for the entire 60 min of reaction time when the dye-to-protein ratio was 100:1 while the average number of labels leveled off at ca.30 min reaction time when the dye-to-protein ratio was 40:1. Apparently, the fluorescent dye available for reaction with lysine was depleted at ca.30 minutes when the dye-to-protein ratio was 40:1, consistent with the kinetics for the competitive hydrolysis reaction. At this point, the total number of dye reacted with mAb1 can be calculated from **Figures 1a and 1b** as 9 labels incorporated per molecule of mAb1. Therefore, when the dye is present at a 40:1 dye-to-protein ratio, the fraction of dye consumed via labeling within 30 minutes is ca. 40%. When the competitive hydrolysis reaction is taken into account, virtually no dye in the ester form is available after 30 min.
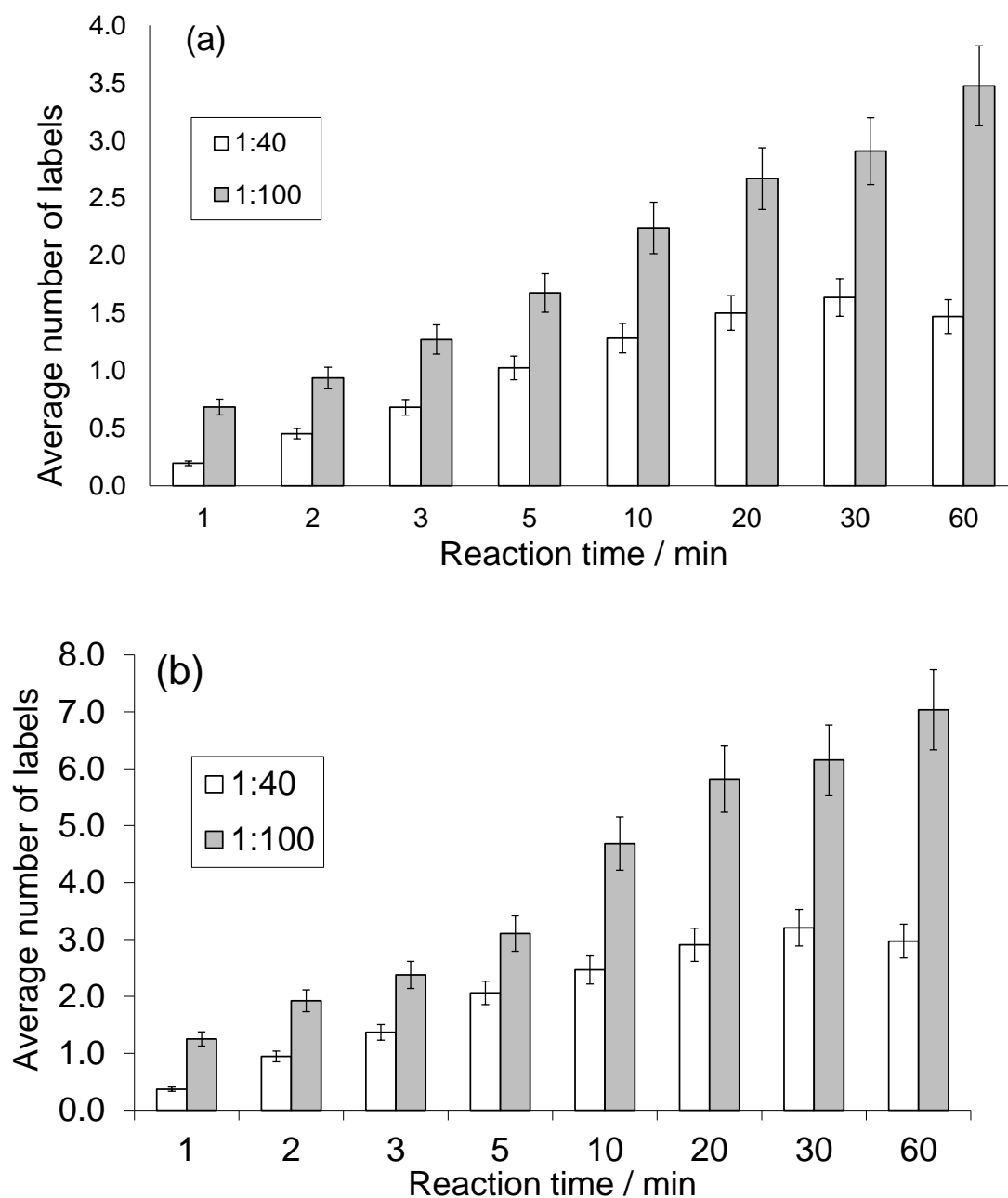
Figure 1. Average number of labels observed at different reaction times for protein-to-dye ratios of 1:40 and 1:100 for mAb-1. The results for light chain (LC) and heavy chain (HC) are shown in 1**a** and 1**b**, respectively. The error bar shows the RSD% values from three experiments.

On the other hand, when the dye-to-protein ratio was 100:1, there is sufficient dye available for reaction with the protein for the entire 60 min of reaction time. Therefore, a target dye-to-protein ratio of 100:1 was chosen in the final method, but it was less critical as long as the ratio remained the same for samples in comparability experiments.

Minimization of labeling time

The fraction of labeled lysine per molecule needs to be controlled at a low level in order to 1.minimize the structural perturbation introduced by the labeling reaction itself, and 2. be able to differentiate the lysines with different solvent accessibilities. For reaction times less than 5 min, <10% of total lysine residues were labeled on each mAb1 molecule. Additionally, the average number of labels incorporated increased at a rather similar rate for both dye-to-protein ratio of 40:1 and 100:1 at short reaction times and the labeling time course results are less sensitive to an accurate measurement of protein concentration within this short reaction time frame. Therefore, a total reaction time of 5 min with 1 min intervals for sampling was selected as the experimental conditions for protein surface lysine labeling.
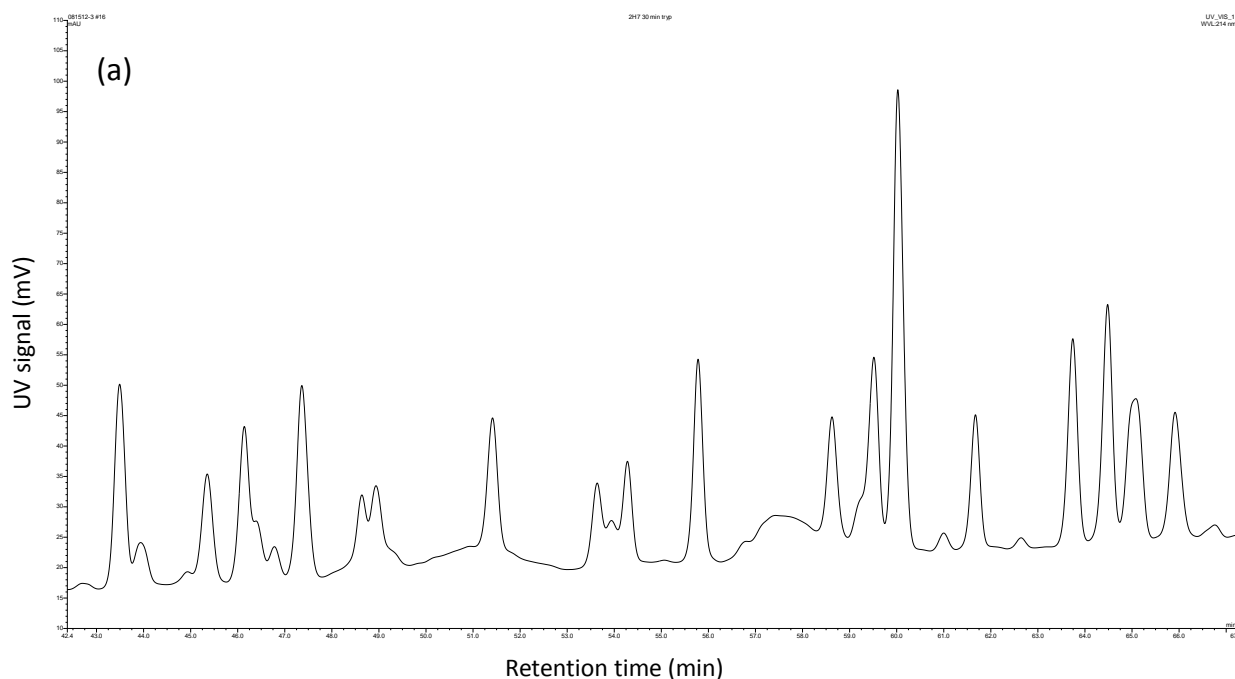
Peptide mapping

The derivatized lysine residues can no longer be cleaved by trypsin. As a result, longer peptides and reduced sequence coverage can be expected if the digestion were to be performed with trypsin alone. Therefore, a combination of Glu-C and trypsin was employed for the digestion step. The extent of mAb1 digestion was measured by examining a partially digested peptide, which eluted at the end of the chromatogram and was recorded during peptide mapping. With the digestion protocol described in the Methods section (see above), the partially digested peptide accounted for <5% of the total peak area (data not shown), indicating rather complete digestion.

The sample digested with Glu-C and trypsin was then analyzed by HPLC-MS/MS and a >90% sequence coverage was achieved. All lysine-containing peptides were observed with high confidence. A list of the identified lysine-containing peptides found in fluorescently labeled mAb1 can be found in the supplementary data (**Table 1**). All but two lysine residues were fluorescently labeled. The two peptides, LC 103-106 and LC 167-169 contained unreacted lysine residues. This may be caused by a lower solvent accessibility, salt bridges with adjacent amino acid residues, or higher than usual pK_a values of the side chain amino groups. The exact reason for the absence of labeling at these two lysines is currently unknown; however, this feature was consistently observed in all our experiments with the mAb1. Importantly, our experimental conditions ensured that, only a single lysine was labeled in all peptides containing multiple lysine residues (**Table 1**). Moreover, it appeared that lysine residues at different positions within these peptides were labeled to a similar extent. Peptides containing multiple lysine residues but with different singly labeled lysine were not resolved by our chromatographic method; however, labeling of the individual lysine residues was confirmed by MS/MS analysis (data not shown).

Table 1. List of identified lysine-containing peptide found in fluorescently labeled mAb-1. The calculated mass, observed mass and mass difference were shown in the table. The observed labeling site(s) and additional modifications were also shown in the table. HC: heavy chain; LC: light chain.

Peptide	Calculated mass/Da	Observed mass/Da	Mass difference (ppm)	Labeling site	Additional modification
Peptides with labeled lysine identified					
HC 39-46	1093.44	1093.44	1.6	HC 43	
HC 47-65	2439.05	2439.05	2.9	HC 63 or HC 65	
HC 68-76	1318.57	1318.58	2.4	HC 74	
HC 75-87	1861.83	1861.84	2.5	HC 76	
HC 127-152	2784.30	2784.30	0.2	HC 38	carboxymethyl
HC 227-238	1574.58	1574.59	3.1	HC 227	
HC 239-253	1890.96	1890.96	2.0	HC 51 or HC 53	
HC 278-288	1649.67	1649.67	0.3	HC 80	
HC 280-293	1971.81	1971.80	-4.9	HC 93	
HC 289-297	1344.62	1344.63	1.3	HC 93 or HC 95	
HC 307-323	2231.06	2231.06	2.2	HC 309 or HC 310	carboxymethyl
HC 324-331	1321.54	1321.53	-2.2	HC 25	carboxymethyl
HC 328-338	1432.65	1432.66	2.5	HC 433	
HC 332-343	1561.77	1561.77	2.6	HC 339 or HC 343	
HC 363-375	1816.81	1816.81	-0.5	HC 365 or HC 375	carboxymethyl
HC 394-406	1757.71	1757.72	3.7	HC 397	
HC 415-421	1112.48	1112.48	1.2	HC 419	
LC 25-44	2574.12	2574.14	6.2	LC 38 or LC 41 or LC 44	
LC 39-60	2514.25	2514.26	6.8	LC 41 or LC 44	
LC 42-60	2232.09	2232.09	1.3	LC 44	
LC 81-104	3166.27	3166.28	2.4	LC 102	carboxymethyl
LC 108-125	2240.03	2240.04	3.0	LC 125	
LC 123-142	2591.17	2591.18	4.9	LC 125	carboxymethyl
LC 143-148	1053.46	1053.46	0.3	LC 144	
LC 145-160	2096.87	2096.88	2.4	LC 148	
LC 169-184	1982.83	1982.83	0.8	LC 182	
LC 170-186	2159.91	2159.91	1.8	LC 182	
LC 187-194	1329.50	1329.50	-0.3	LC 187 or LC 189	carboxymethyl
LC 195-210	2051.94	2051.94	3.5	LC 206	
Peptides with unlabeled lysine identified					
LC 103-106	487.30	487.30	1.5		
LC 167-169	1716.88	1716.88	0.4		

The UV-trace of fluorescently labeled mAb 1 peptide map shows significantly more peaks than usually expected in a typical peptide map of a monoclonal antibody. The increased number of peaks is due to (i) the presence of peptides with and without lysine labeling, (ii) the effect of lysine-labeling on tryptic digestion, and (iii) missed cleavages mainly by Glu-C. Not all peaks were baseline-resolved and the characterization of all peaks would take a significant amount of time. On the other hand, observe the map with the fluorescent detector offers a much cleaner view, showing only the peptides that contain lysine residues labeled with the fluorescent dye. These peaks can be identified by mass spectrometric analysis and the corresponding UV peaks can then be identified from their same retention times. The fluorescence peak area can also be automatically measured as all fluorescence peaks are baseline-resolved with good signal-to-noise ratio. A Typical peptide maps of mAb1 with labeled lysines can be found in supplementary data (**Figure 2a** (UV-detection at 214 nm) and **Figure 2b** (fluorescence detection, λ_{exc} =350nm/λ_{em} = 490nm)). Only the retention time window from 42 to 67 min is displayed in these figures.
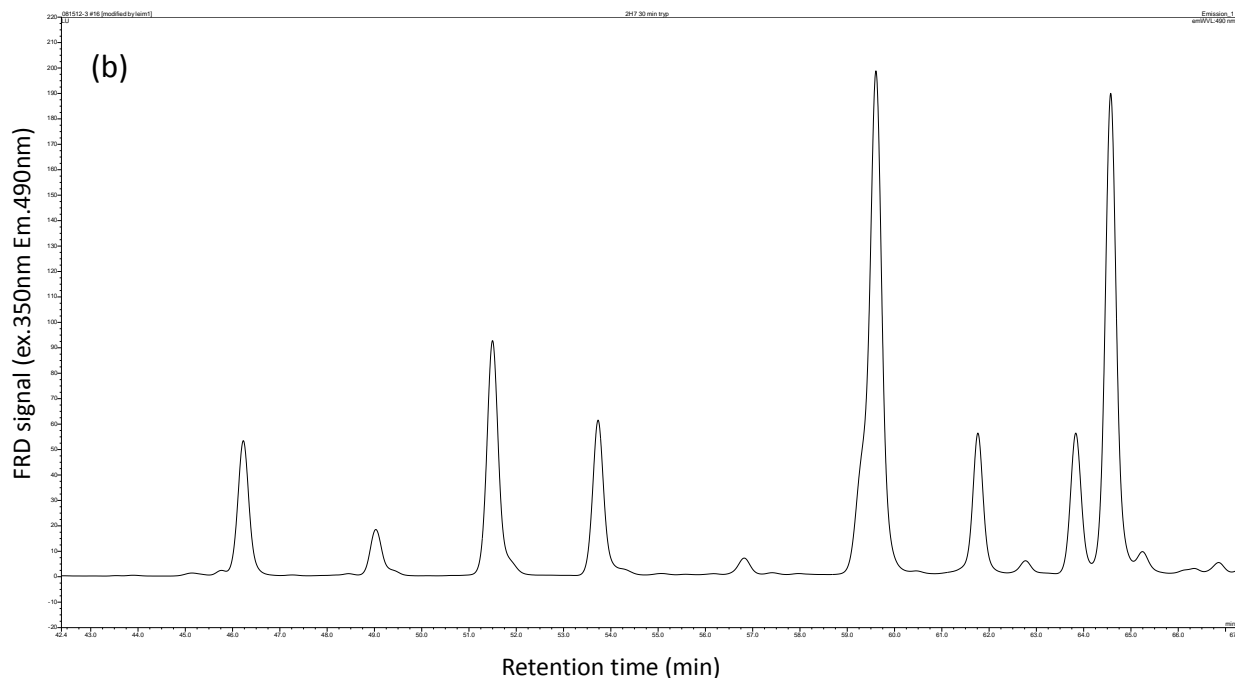
Figure 2. Typical chromatograms of a mAb1 tryptic + Glu-C digest observed monitored by UV (**a**) and fluorescence (**b**) detection. The chromatogram was zoomed-in to retention times between 42 and 67 min. The UV detector wavelength was 214 nm while the excitation and emission wavelengths for the fluorescent detector were set at 350nm and 490 nm, respectively.

Relative quantitation

Since there are multiple steps involved in sample preparation, the degrees of recoveries of the different steps are reflected in the fluorescence peak area (A_{FR}). The direct measurement of protein concentration after lysine labeling was not feasible due to the absorbance of the fluorescent dye at 280 nm. Therefore, the UV peak areas recorded at 214 nm of three non-lysine-containing peptides were used to determine protein concentration in each sample. As these peptides do not contain lysine, their UV absorption is not contaminated by dye absorption, and is proportional to their abundance. Additionally, these peaks are well-resolved from adjacent peaks. An arbitrary protein concentration can be assigned to one of the samples and the protein concentrations of all other samples can be normalized to this value. The UV peak area (A_{UV}) was

measured for each of the three peptides and the ratio of A_{FR} and A_{UV} was calculated. The average value of this ratio was used to normalize fluorescence peak area. The normalized fluorescence peak area (A^0_{FR}) was used to represent the fluorescent labeling level of that peptide. The term A^0_{FR} and fluorescent labeling level will be used interchangeably in this paper. The calculation of A^0_{FR} for peak I follows the expression below:

$$A^0_{FR_i} = \frac{A_{FR_i}}{average \; \frac{A_{FR}}{A_{UV}} \; value \; of \; three \; non-lysine \; containing \; peptides}$$

The reproducibility of this method was assessed with triplicate experiments. The normalized fluorescence peak areas were also calculated and the RSD% value for these three experiments were <10%. The level of missed cleavages was carefully examined both qualitatively and quantitatively for each experiment and was deemed constant.

Structural Changes Induced by Deglycosylation

Previous NMR and H/DX-MS[24,39] experiments have revealed that IgG1 undergoes multiple structural changes upon deglycosylation. These structural changes are mainly located in the CH2 and CH3 domains of the Fc region. The NMR method demonstrated that residues that showed chemical shift differences were located on the opposite side of the glycosylation site in the CH2 and CH3 domains. Instead, the HDX-MS method revealed a more wide-spread difference in H/D exchange throughout the Fc region. The chemical shift differences observed by NMR and differences in H/D exchange rates are both indicators of protein structural changes. Since this fluorescent labeling method is set up to experimentally access the solvent accessibility of surface lysines, it should be able to reveal structural differences between native and deglycosylated mAb1.

The mAb1 used in the present study is an IgG1 molecule with N-glycosylation at N305 on both heavy chains. To compare the structural changes upon deglycosylation, mAb1 was subjected to PNGase F treatment as described above. The complete removal of the N-glycan was confirmed by ESI-MS analysis (data not shown). It was reported that the removal of N-glycans can sometimes lead to dimerization[40,41]. Therefore, the levels of dimers for both native and deglycosylated mAb1 were monitored by size-exclusion chromatography (data not shown). The dimer levels in both samples were comparable, 0.7% for native and 0.8% for deglycosylated mAb1, demonstrating that the removal of N-glycan from mAb1 did not significantly increase dimer levels. Subsequently, both native and deglycosylated mAb1 were subjected to fluorescence labeling with Alexa Fluor 350 SE and peptide mapping. Chromatograms of the digested samples were monitored both by UV and fluorescence detection, and individual peaks were analyzed by HPLC-MS/MS. Normalized fluorescence peak areas (A^0_{FR}) were calculated using the formula described above.

The A^0_{FR} for labeled native and deglycosylated mAb1 after 5 min reaction time are shown in a mirror plot in **Figure 3**. Only the peptides monitored by fluorescence detection are plotted and consecutively numbered according to their retention times. The normalized fluorescence peak areas are different for lysine residues at different locations on the mAb1, indicating that they exhibit different reactivity with the fluorescent dye. By comparing the normalized fluorescence peak areas of native and deglycosylated mAb1, we can identify the lysine-containing peptides that experience structural change induced by deglycosylation. A visual comparison of the normalized fluorescence peak areas in **Figure 3** reveals a major difference of the labeling efficiency for peptide 21.
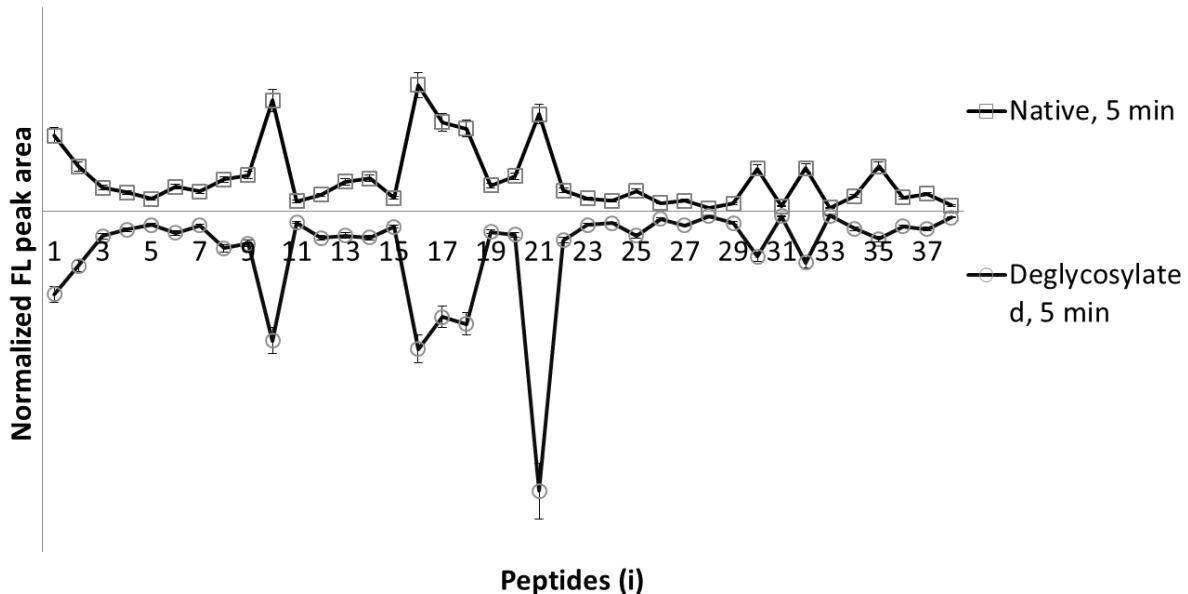
Figure 3. Mirror plot of the lysine-containing peptides from native (upper) and deglycosylated (lower) mAb1 with derivatized by surface lysine fluorescence labeling. Labeling was performed at a protein-to-dye ratio of 1:100 with a labeling time of 5 min. The fluorescence peak area of each peak was normalized to the protein concentration of the sample. The peptides are numbered according to their retention times. The error bar shows the RSD% values from three experiments.

The A^0_{FR} of the deglycosylated sample was significantly larger than that of native sample for this peptide. To analyze for minor differences, the $\%A^0_{FR}$ difference for each peptide i can be calculated based on equation (1):

$$\%\text{A}^0_{FR}\ difference_i = \frac{A^0_{FR,deglycosylated,i} - A^0_{FR,native,i}}{A^0_{FR,native,i}} \times 100\% \qquad (1)$$

The $\%A^0_{FR}$ difference for each fluorescently labeled peptide is displayed in **Figure 4**. The two bold lines in **Figure 4** indicate a ±3RSD% difference. A percent A^0_{FR} difference greater than

±3RSD% was considered significant. The difference for most of the peptides was within assay variability, indicating limited structural changes upon deglycosylation. This observation is qualitatively consistent with the published NMR and HDX-MS data on IgG1. Only a few peptides showed a $\%A^0_{FR}$ difference greater than 3RSD%.
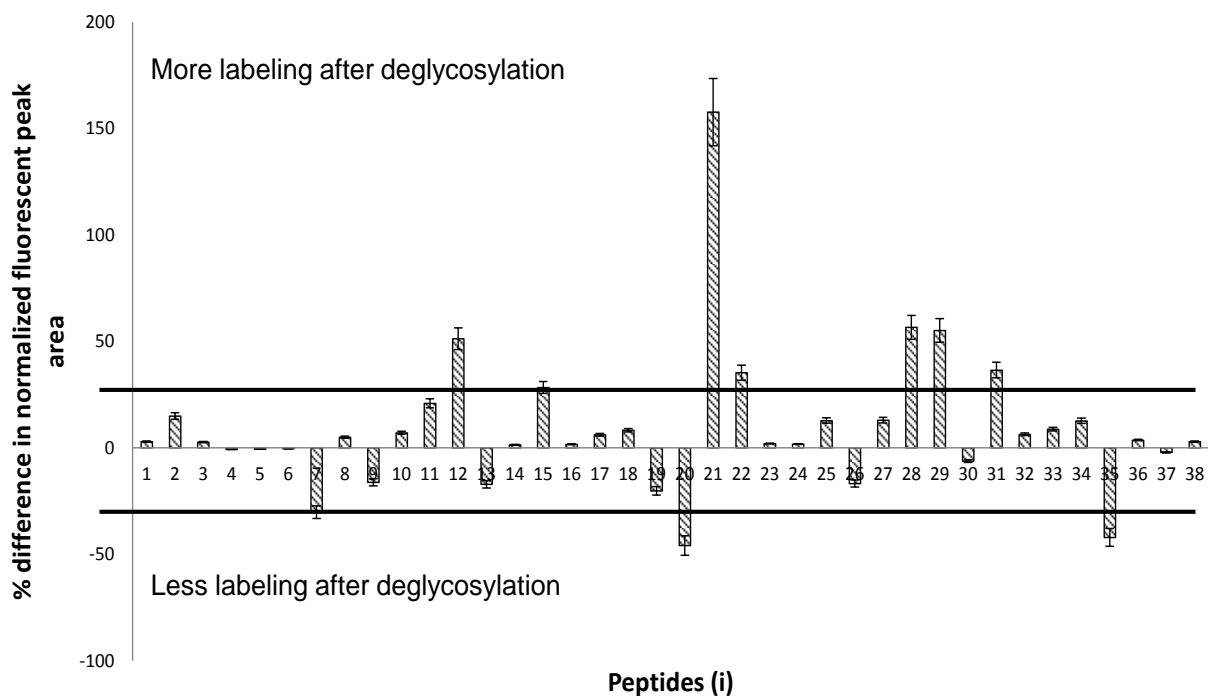

Figure 4. Bar chart showing the percent difference between normalized fluorescence peak area of lysine-containing peptides from native and deglycosylated mAb1 derivatized by surface lysine fluorescent labeling. The peptides are numbered according to their retention times. Labeling was performed at a protein-to-dye ratio of 1:100 with a labeling time of 5 min. The ± 3 RSD% levels of this experiment are marked with a bold line. Percent difference greater than 3 RSD% was deemed as significant. The error bar shows the RSD% values from three experiments.

The locations of these peptides on a mAb1 homology structure are displayed in **Figure 5**. Among these, peptide 21 showed the most significant change in A^0_{FR}. The locations of lysines and the N-glycosylation site are color-coded in Figure 5, while the glycan structures are not shown. The labeling efficiency for most of the lysine residues remained unchanged upon deglycosylation. The lysine residues with an increased labeling efficiency after deglycosylation are K251, K253, K365 and K375, all of which are located on the HC of mAb1. Peptide 21, containing K251 and K253, showed a ca.4-fold increase of lysine labeling after deglycosylation. These two lysine residue are located in the CH2 domain of mAb1, for which NMR and H/DX-MS revealed increased solvent accessibility upon deglycosylation. On the other hand, the labeling efficiency of K365 (peptides 28 and 29) and K375 (peptides 12 and 31) increased only moderately (ca. 30%). These two lysine residues are located in the CH3 domain of mAb1.H/DX-MS analysis revealed a similar result while NMR analysis showed no significant difference of solvent accessibility difference in for this region. On the LC, K125 (peptides 20 and 35) suffered a ca.30% reduction of labeling upon deglycosylation. This peptide is located relatively far away from the N-glycosylation site showing that deglycosylation may induce long-distance structural or dynamic changes. Interestingly, the two K125 residues on both light chains are located in close distance from each other (**Figure 6**). These lysine residues are also located next to acidic residues, D and E, which are negatively charged under our experimental conditions (pH 7.5). Upon deglycosylation, a slight structural change could result in increased electrostatic interactions between positively charged K and negatively charged D and E. An increased electrostatic interaction may shorten the distance between the two halves of the antibody, or slow down the conformational dynamics (e.g. opening and closing of this local domain). As a result, the labeling efficiency of these two lysine residues can decrease upon deglycosylation. The exact

cause for the reduced labeling of K125 was out of the scope of this work and was not further pursued.
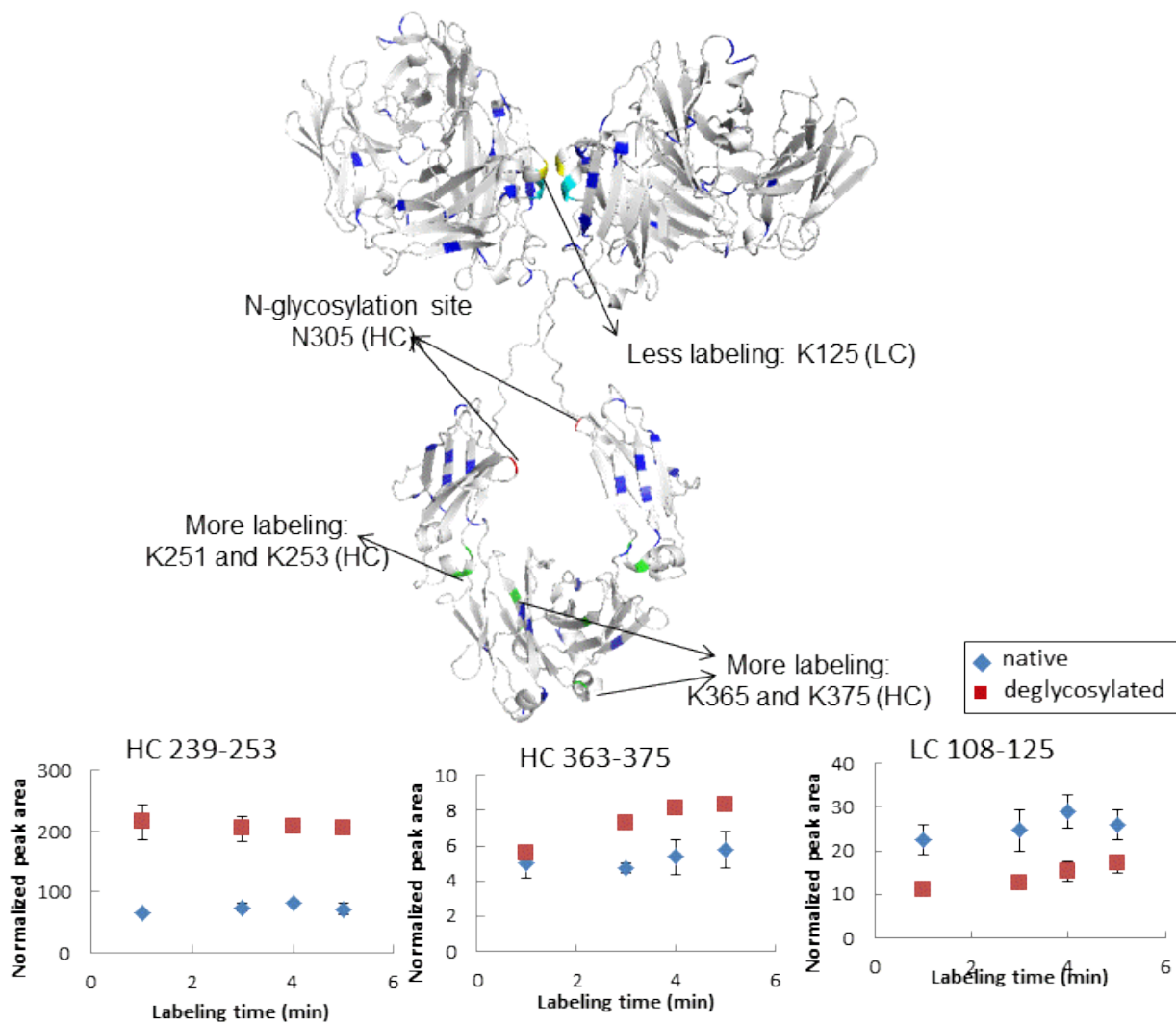

Figure 5. Homology structure of mAb1 showing the lysine residues and N-glycosylation site (side view). The lysine residues with an unchanged level of fluorescence labeling upon deglycosylation are colored blue, lysine residues with increased levels of fluorescence labeling upon deglycosylation are colored green, while lysine residues with decreased levels of

fluorescence labeling upon deglycosylation are colored yellow. The N-glycosylation site is colored red. The glycan structures are not shown. Time courses showing peptides with differences in fluorescence labeling are shown on the bottom.
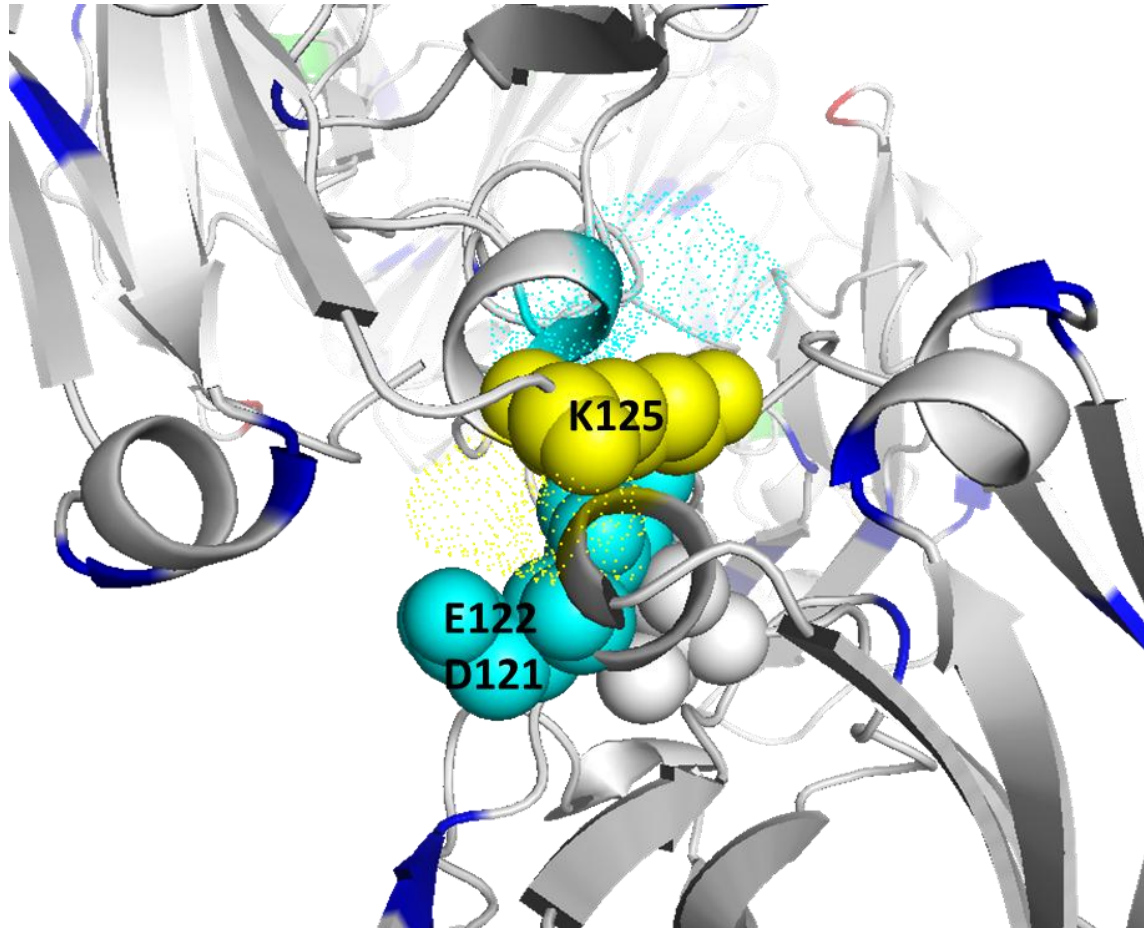

Figure 6. Homology structure of mAb1 showing the lysine residues with decreased levels of fluorescent labeling (HC K125) upon deglycosylation (top view). Neighboring acidic amino acids (E and D) are colored cyan. These residues are shown as spheres. Otherwise, the color scheme is the same as in **Figure 5**.

The locations of lysine residues with significant differences in labeling efficiency represent locations where deglycosylation significantly changes the reactivity with the labeling reagent. This change of reactivity most likely correlates with increased solvent accessibility. Our results generally agree with published data in that only limited structural change is observed upon deglycosylation of IgG1. The small differences between the exact locations of structural changes at the amino acid level between our data and the work of others may result from the use of different techniques (labeling of K vs. NMR and H/DX-MS), a different sequence of our mAb1 and different experimental conditions (pH). In addition, surface lysine labeling monitors structural differences experienced by the amino acid side chain rather than the backbone, which is monitored by H/DX-MS.

The new methodology described here is able to identify structural changes at the peptide level. The main advantage of our method is the short sample preparation protocol and a straight-forward data analysis. Data analysis is based on chromatographic peak areas with good resolution and S/N. Therefore, our method can be applied in a high throughput manner with no specialized software. With respect to quantitative analysis, the measurement of chromatographic peak areas is more accurate when compared to a MS signal-based technique, which may suffer from differences in ionization efficiencies for different peptides and ion suppression from impurities.

Plots for reaction times between 1 and 5 min were obtained to confirm the observed $\%A^0_{FR}$ differences. These time course plots can also be used to rule out abnormal $\%A^0_{FR}$ differences potentially caused by experimental errors at specific time points. The A^0_{FR} time course plots of all identified lysine-containing peptides are shown in the Supplementary Material (**Figure S1**).

The %RSD values from three independent experiments are shown as error bars in each plot. Many of the peptides containing overlapping sequences (e.g. LC 108-125 and LC 123-142, LC 39-60 and LC 42-60, HC 68-76 and HC 75-87, HC 278-288 and HC 280-293, HC 328-338 and HC 332-343) showed similar trends. The results from these overlapping peptides offered an additional opportunity to confirm our results.

The Effect of PS-20 on mAb1 Structure

PS-20 is a non-ionic surfactant commonly used as an excipient in therapeutic protein products. It is usually present at 0.01%-0.1% (w/w) to protect proteins from surface adsorption, aggregation and denaturation caused by sheer forces during shipping[34,35,42,43]. The interaction between PS-20 and proteins has been studied by various techniques such as CD spectroscopy, isothermal titration calorimetry (ITC) and tryptophan fluorescence[44-47]. These experiments demonstrated that PS-20 interacted with proteins in a non-specific manner and that the interaction was generally weak. On the other hand, the effect of PS-20 on protein stability was apparently dependent on the PS-20 to protein ratio. The exact effect of PS-20 as a protein protector varies from protein to protein. Deechongkit *et al.* [44] demonstrated a PS-20-dependent global protein structural change for an alpha helix-rich monomeric protein (Darbepoetin alfa). However, more specific information on the peptide and/or amino acid level was not obtained due to the limited resolution of the analytical methods (CD and tryptophan fluorescence). Previous findings indicated that the interaction between PS-20 and IgG is negligible[46,47]. Here, we will apply fluorescent surface lysine labeling to study the interaction between PS-20 and mAb1 at various PS-20 to protein ratios.

Our mAb1 (5 mg/mL) was incubated with 0.01%-0.5% PS-20 such that the protein-to-PS-20

ratio was approximately 1:3, 1:10, 1:30 and 1:100. Both the protein concentration and PS-20

concentration range are typical for therapeutic protein formulations. PS-20 does not affect the

chemical reactions that are important for our method and was, therefore, not removed before

fluorescent labeling. The protein sample containing PS-20 was subjected to fluorescent labeling,

denaturation and digestion according to the protocols described in the experimental section

above. The protein-to-dye ratio was 1:100 and five time points for each sample were collected

for 1-5 min of reaction time. The A^0_{FR} was calculated as described above. Three independent

samples were prepared for each of the experiments shown below.

The normalized fluorescent peak areas (A^0_{FR}) obtained from various PS-20 concentrations are

compared in **Figure 7**. Overall, the fluorescent labeling does not change significantly for protein-

to-PS-20 ratios between 1:3 and 1:100 while some difference were noted for mAb1 in the

absence and presence of PS-20 (e.g., peptides 11, 16, 24 and 33). There is no clear PS-20

concentration-related trend observed in this experiment. These data suggest that the interaction

between PS-20 and mAb1 is comparable for protein to PS-20 ratios between 1:3 and 1:100. This

observation is different compared to that made for Darbepeotin alpha, where a protein-to-PS-20

ratio of 1:15 had the strongest stabilizing effect[44]. The difference could be due to the fact that

Darbepeotin is mainly composed of α-helix while mAb1 contains mainly β-sheets. Previous

reports found that only monomeric PS-20 rather than micelles are responsible for the interaction

between PS-20 and proteins[44]. Since the PS-20 concentrations used in our experiments were all

above the critical micelle concentration (CMC), the concentration of PS-20 monomers was

relatively small and constant while the concentration of PS-20 micelles increased with PS-20

concentration. The absence of a clear trend between protein to PS-20 ratios of 1:3 and 1:100 would argue against a strong interaction of PS-20 micelles with our mAb1.
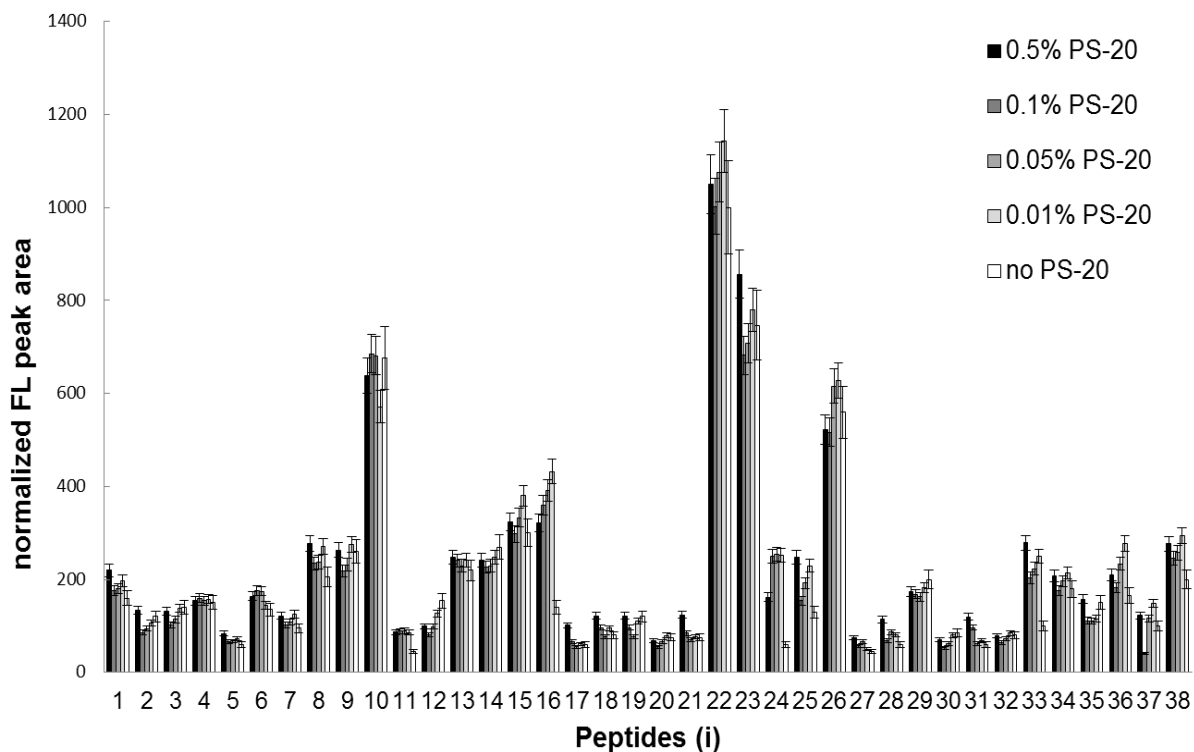

Figure 7. Bar chart showing the normalized fluorescence peak areas of labeled mAb1 peptides in the presence of 0-0.5% PS-20. The protein concentration was constant at 5 mg/mL. The peptides are numbered according to their retention times. The error bar shows the RSD% values from three experiments.

The A^0_{FR} for mAb1 peptides in the presence and absence of PS-20 were compared. The PS-20 concentration representatively compared here was 0.01% since this is a typical concentration

used in formulations for biotherapeutics. The lysine residues with an increased A^0_{FR} were

marked with magenta on the homology structure in **Figure 8**. No lysine residues were observed

with a decreased level of fluorescence labeling. Lysine residues with an unchanged level of

fluorescence labeling were not colored. Since PS-20 is a non-ionic surfactant, the interaction

between PS-20 and the mAb1 is mainly between the hydrophobic regions of the protein and the

hydrocarbon chains of PS-20[45]. The hydrophobic residues on mAb1, namely V, I, L, M, F and

W, are colored orange for comparison in the same Figure 8. Most of the lysine residues with an

increased level of fluorescence labeling are located in proximity to the hydrophobic pockets of

mAb1. Among these, three lysine residues are located in the VL domain, two in the VH domain,

two in the CL domain, one in the CH1 domain and two in the CH3 domain. The locations of

these lysine residues spread across the entire IgG1 structure indicating that the interaction

between PS-20 and mAb1 is not specific. The increased level of fluorescence labeling suggests

that the presence of PS-20 increased the reactivity of the lysine residue under consideration. This

observation may due to 1. an increased solvent accessibility of the lysines in these regions as PS-

20 stabilizes the interaction between these hydrophobic region and the aqueous environment. 2.

an increased local dye concentration in the non-polar phase of the PS-20 layer, leading to an

increased local dye-to-protein ratio in these hydrophobic regions. The lysine reaction time

courses, indicating a PS-20-dependent increase of fluorescence labeling, are shown on the

bottom of **Figure 8**. Only the peptides with fluorescence labeling efficiency difference greater

than 30% were shown in the figure. Overall, the differences between the fluorescence labeling in

the presence and absence of PS-20 is relatively small. The differences in fluorescence labeling

were mostly <30% at the end of the 5 min reaction time and differences were generally not

apparent before 3 min of reaction time. These growing differences may indicate that the interaction between PS-20 and protein affects the protein dynamics in these regions.
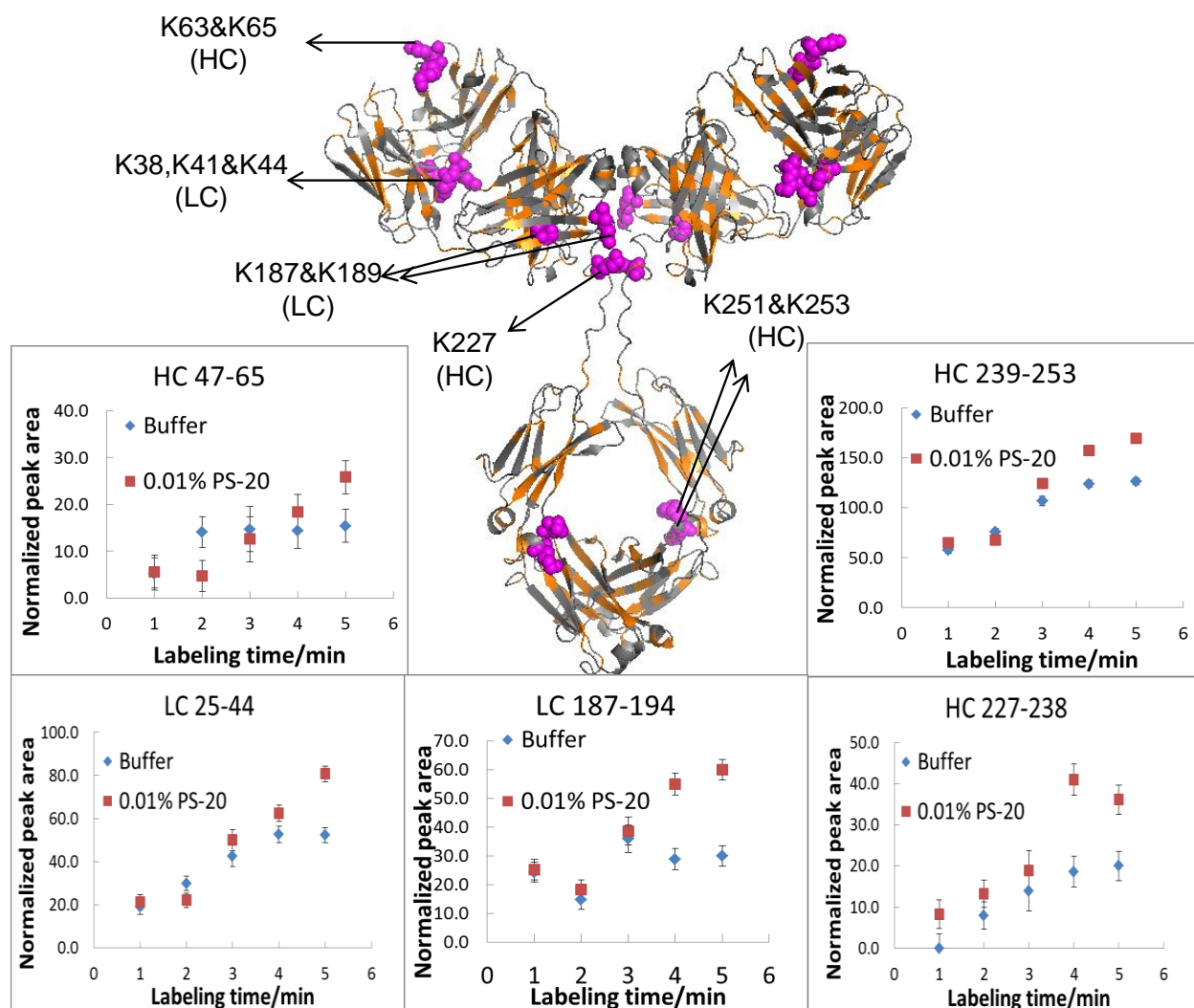

Figure 8. Homology structure of mAb1 showing hydrophobic residues and the lysine residues with increased levels of fluorescence labeling in the presence of 0.01% PS-20. The hydrophobic residues are colored orange. Lysine residues with increased levels of fluorescence labeling ware colored magenta. Lysine residues with changed labeling levels are highlighted in the homology structure (only half of the lysines are highlighted due to structural symmetry). Plots of time

courses showing peptides with differences in fluorescence labeling are shown on the bottom. The error bar shows the RSD% values from three experiments.

 Overall, our results are consistent with the notion that the interaction between PS-20 and mAb1 is generally weak. Most of the lysine residues did not show any significant differences in fluorescence labeling. For those lysine residues which showed a difference, this difference was <30% (RSD% < 10%). The presence of PS-20 increased the fluorescence labeling of several lysine residues on the mAb1. These lysine residues are located near regions of relatively high hydrophobicity. A protein-to-PS-20 ratio ranging from 1:3 to 1:100 does not appear to affect the interaction of PS-20 with our mAb1.

The sample preparation and analysis requires no specialized instruments, while the data analysis can be done automatically in batch mode. The high throughput nature of this method makes it a very useful screening tool.

CONCLUSIONS

The surface lysine fluorescent labeling method described here utilizes a fluorescent dye to probe the solvent accessibility of protein surface lysines. The solvent accessibility changes can represent protein structural and dynamic differences. We demonstrated that this method is capable of detecting structural changes on a monoclonal antibody. The introduction of fluorescent labeling makes it possible to detect changes in lysine reactivity, which correlates with solvent accessibility. The fluorescence detection is sensitive with a wide dynamic range. This method can be used to screen multiple different excipients to get an overview of their interaction with a protein within a few days. Alternatively, when a conformational difference between two

samples is suspected, this method can rapidly provide results to guide a decision on whether to invest resources to analyze these differences by more sophisticated techniques. Once a difference in fluorescence labeling has been confirmed by chromatography, an HPLC-MS/MS experiment can be performed to identify the exact location of this difference. The fluorescent dye used here does not interfere with the MS signal and the data analysis step can be achieved with commonly used software such as Mascot (Matrix Science) or Proteome Discoverer (Thermo Scientific). The chromatography peak area based calculation is reproducible and automatable. When studying the comparability of multiple samples, this method can potentially be used in a high throughput manner screening for structural differences between samples without the need of extensive data mining.

REFERENCES

(1) Mann, M.; Jensen, O. N. *Nat. Biotechnol.* **2003**, *21*, 255-261.

(2) Schulz, G. E., Schirmer, R. H. *Principles of protein structure.*: Springer-Verlag KG., 1979.

(3) Henzler-Wildman, K.; Kern, D. *Nature* **2007**, *450*, 964-972.

(4) Deechongkit, S.; Aoki, K. H.; Park, S. S.; Kerwin, B. A. *J. Pharm. Sci.* **2006**, *95*, 1931-1943.

(5) Chirino, A. J.; Mire-Sluis, A. *Nat Biotech* **2004**, *22*, 1383-1391.

(6) US Fed. Reg., pp 37861-37862.

(7) Rathore, A. S.; Winkle, H. *Nat Biotech* **2009**, *27*, 26-34.

(8) Huang, J.; Kaul, G.; Cai, C.; Chatlapalli, R.; Hernandez-Abad, P.; Ghosh, K.; Nagi, A. *Int. J. Pharm.* **2009**, *382*, 23-32.

(9) Wang, Y.; Lu, Q.; Wu, S.-L.; Karger, B. L.; Hancock, W. S. *Anal. Chem.* **2011**, *83*, 3133-3140.

(10) Essex, D.; Chen, K.; Swiatkowska, M. *Localization of protein disulfide isomerase to the external surface of the platelet plasma membrane*, 1995; Vol. 86, p 2168-2173.

(11) Travaglini-Allocatelli, C.; Ivarsson, Y.; Jemth, P.; Gianni, S. *Current Opinion in Structural Biology* **2009**, *19*, 3-7.

(12) Bax, A. *Protein Sci.* **2003**, *12*, 1-16.

(13) Wishart, D. S.; Sykes, B. D.; Richards, F. M. *Biochemistry* **1992**, *31*, 1647-1651.

(14) Brunger, A. T.; Adams, P. D.; Clore, G. M.; DeLano, W. L.; Gros, P.; Grosse-Kunstleve, R. W.; Jiang, J.-S.; Kuszewski, J.; Nilges, M.; Pannu, N. S.; Read, R. J.; Rice, L. M.; Simonson, T.; Warren, G. L. *Acta Crystallographica Section D* **1998**, *54*, 905-921.

(15) Svergun, D. I.; Petoukhov, M. V.; Koch, M. H. J. *Biophys. J.* **2001**, *80*, 2946-2953.

(16) Arrondo, J. L. R.; Young, N. M.; Mantsch, H. H. *Biochimica et Biophysica Acta (BBA) - Protein Structure and Molecular Enzymology* **1988**, *952*, 261-268.

(17) Dzwolak, W.; Smirnovas, V.; Jansen, R.; Winter, R. *Protein Sci.* **2004**, *13*, 1927-1932.

(18) Surewicz, W. K.; Mantsch, H. H.; Chapman, D. *Biochemistry* **1993**, *32*, 389-394.

(19) Chang, C. T.; Wu, C.-S. C.; Yang, J. T. *Anal. Biochem.* **1978**, *91*, 13-31.

(20) Sreerama, N.; Venyaminov, S. Y.; Woody, R. W. *Anal. Biochem.* **2000**, *287*, 243-251.

(21) Berkowitz, S. A.; Engen, J. R.; Mazzeo, J. R.; Jones, G. B. *Nat Rev Drug Discov* **2012**, *11*, 527-540.

(22) Houde, D.; Arndt, J.; Domeier, W.; Berkowitz, S.; Engen, J. R. *Anal. Chem.* **2009**, *81*, 2644-2651.

(23) Houde, D.; Berkowitz, S. A.; Engen, J. R. *J. Pharm. Sci.* **2011**, *100*, 2071-2086.

(24) Englander, J. J.; Del Mar, C.; Li, W.; Englander, S. W.; Kim, J. S.; Stranz, D. D.; Hamuro, Y.; Woods, V. L. *Proceedings of the National Academy of Sciences* **2003**, *100*, 7057-7062.

(25) Konermann, L.; Tong, X.; Pan, Y. *J. Mass Spectrom.* **2008**, *43*, 1021-1036.

(26) Manikwar, P.; Majumdar, R.; Hickey, J. M.; Thakkar, S. V.; Samra, H. S.; Sathish, H. A.; Bishop, S. M.; Middaugh, C. R.; Weis, D. D.; Volkin, D. B. *J. Pharm. Sci.* **2013**, *102*, 2136-2151.

(27) Zhang, Z.; Smith, D. L. *Protein Sci.* **1993**, *2*, 522-531.

(28) Maleknia, S. D.; Chance, M. R.; Downard, K. M. *Rapid Commun. Mass Spectrom.* **1999**, *13*, 2352-2358.

(29) Sharp, J. S.; Becker, J. M.; Hettich, R. L. *Anal. Biochem.* **2003**, *313*, 216-225.

(30) Wang, L.; Chance, M. R. *Anal. Chem.* **2011**, *83*, 7234-7241.

(31) Zhang, H.; Gau, B. C.; Jones, L. M.; Vidavsky, I.; Gross, M. L. *Anal Chem* **2011**, *83*, 311-318.

(32) Zhang, L.; Lilyestrom, W.; Li, C.; Scherer, T.; van Reis, R.; Zhang, B. *Anal. Chem.* **2011**, *83*, 8501-8508.

(33) Chi, E. Y.; Krishnan, S.; Randolph, T. W.; Carpenter, J. F. *Pharm. Res.* **2003**, *20*, 1325-1336.

(34) Katakam, M.; Bell, L. N.; Banga, A. K. *J. Pharm. Sci.* **1995**, *84*, 713-716.

(35) Krielgaard, L.; Jones, L. S.; Randolph, T. W.; Frokjaer, S.; Flink, J. M.; Manning, M. C.; Carpenter, J. F. *J. Pharm. Sci.* **1998**, *87*, 1593-1603.

(36) Mahler, H.-C.; Müller, R.; Frie, W.; Delille, A.; Matheus, S. *European Journal of Pharmaceutics and Biopharmaceutics* **2005**, *59*, 407-417.

(37) Duncan, M. R.; Lee, J. M.; Warchol, M. P. *Int. J. Pharm.* **1995**, *120*, 179-188.

(38) Lewis, M. R.; Kao, J. Y.; Anderson, A.-L. J.; Shively, J. E.; Raubitschek, A. *Bioconjugate Chem.* **2001**, *12*, 320-324.

(39) Yamaguchi, Y.; Nishimura, M.; Nagano, M.; Yagi, H.; Sasakawa, H.; Uchida, K.; Shitara, K.; Kato, K. *Biochimica et Biophysica Acta (BBA) - General Subjects* **2006**, *1760*, 693-700.

(40) Krapp, S.; Mimura, Y.; Jefferis, R.; Huber, R.; Sondermann, P. *J. Mol. Biol.* **2003**, *325*, 979-989.

(41) Kayser, V.; Chennamsetty, N.; Voynov, V.; Forrer, K.; Helk, B.; Trout, B. L. *Biotechnology Journal* **2011**, *6*, 38-44.

(42) Jones LaToya, S.; Bam Narendra, B.; Randolph Theodore, W. In *Therapeutic Protein and Peptide Formulation and Delivery*; American Chemical Society, 1997, pp 206-222.

(43) Kerwin, B. A. *J. Pharm. Sci.* **2008**, *97*, 2924-2935.

(44) Deechongkit, S.; Wen, J.; Narhi, L. O.; Jiang, Y.; Park, S. S.; Kim, J.; Kerwin, B. A. *J. Pharm. Sci.* **2009**, *98*, 3200-3217.

(45) Randolph, T.; Jones, L. In *Rational Design of Stable Protein Formulations*, Carpenter, J.; Manning, M., Eds.; Springer US, 2002, pp 159-175.

(46) Garidel, P.; Hoffmann, C.; Blume, A. *Biophys. Chem.* **2009**, *143*, 70-78.

(47) Hoffmann, C.; Blume, A.; Miller, I.; Garidel, P. *European Biophysics Journal* **2009**, *38*, 557-568.

SUPPLIMENTARY DATA

FIGURE CAPTIONS FOR SUPPLIMETRAY DTA

Figure S1. Normalized FL peak area of lysine-containing peptides from native and deglycosylated mAb-1 with surface lysine fluorescent labeling with 1-5 min reaction time. The error bar represents the standard deviation calculation from three repetitive experiments. The FL peak area of each peak was normalized to the protein concentration of the sample.

Figure S2. Normalized FL peak area of lysine-containing peptides from mAb-1 in buffer and 0.01% PS-20 with 1-5 min reaction time. Only data from the peptides with a significant fluorescent labeling level difference were shown. The error bar represents the standard deviation calculation from three repetitive experiments. The FL peak area of each peak was normalized to the protein concentration of the sample.

Figure S1

HC 68-76

HC 75-87

HC 127-152

HC 227-238

HC 280-293

HC 289-297

HC 307-323

HC 324-331

HC 363-375

HC 394-406

HC 415-421

LC 25-44

LC 39-60

LC 42-60

LC 81-104

LC 108-125

LC 123-142

LC 143-148

LC 145-160

LC 170-186

LC 187-194

LC 195-210